HTML ABSTRACT + LINKS

The multiconfiguration time-dependent Hartree–Fock method for quantum chemical calculations

M. Nest, T. Klamroth, and P. Saalfrank
Institut für Chemie, Universität Potsdam, Karl-Liebknecht-Strasse 24–25, 14476 Potsdam, Germany

(Received 15 November 2004; accepted 4 January 2005; published online 28 March 2005)

We apply the multiconfiguration time-dependent Hartree–Fock method to electronic structure calculations and show that quantum chemical information can be obtained with this explicitly time-dependent approach. Different equations of motion are discussed, as well as the numerical cost. The two-electron integrals are calculated using a natural potential expansion, of which we describe the convergence behavior in detail. © *2005 American Institute of Physics*. [DOI: 10.1063/1.1862243]

I. INTRODUCTION

Until recently, quantum chemical calculations dealt, in its majority, with the solution of the time-independent Schrödinger equation. For this purpose a vast collection of techniques has been accumulated. In this paper we propose to make use of some of these techniques, the complete active space self-consistent field (CASSCF) scheme, to solve the time-*dependent* Schrödinger equation (TDSE). These solutions, usually time-dependent wave packets $\Psi(t)$, can give answers to quantum chemical problems in a way which complements and extends the standard approach. Furthermore, this *ansatz* offers a way to describe systems of electrons out of equilibrium. For example, laser induced electron dynamics, or the relaxation of an excited electron configuration can be studied in detail.

Most of the explicitly time-dependent approaches to quantum chemistry yet, were carried out either on the density functional (TD-DFT),[1,2] or the Hartree–Fock (TD-HF) level of theory.[3,4] There is often a confusion attached to these abbreviations because they are often used for time-independent, linear-response calculations. One drawback of time-dependent HF/DFT calculations is that they are basically one determinant approaches. This means that correlation is scarcly accounted for. One of us (T.K.) introduced recently the time-dependent analog of the configuration interaction (CI) methods,[5] which is a systematically improvable *ansatz* for laser driven quantum dynamics of electrons. With CI, only the coefficients of the determinants are optimized. In this paper we want to study the multiconfiguration time-dependent Hartree–Fock (MCTDHF) method, which optimizes the orbitals as well, and is thus very economic. It can either be seen as an explicitly time-dependent version of the CASSCF methods,[6] or a specialization of the well established MCTDH (Refs. 7–10) method for (distinguishable) nuclei to (indistinguishable) fermions. Its particular advantage lies in the variational optimization of coefficients *and* orbitals at the same time. Independent of our own work, there have been a couple of very recent applications of MCTDHF by other groups, specifically in the field of strong laser-electron interactions and ionization.[11,12] It is the purpose of this paper to study its suitability for electronic structure calculations.

The TDSE is usually solved either with respect to a real time variable t, or an imaginary time variable $\tau=it$. The latter is a frequently used way to compute the ground state (and occasionally excited states[13]) in nuclear quantum dynamics. It is one of the purposes of this paper to present systematic tests of the suitability of the MCTDHF propagation in imaginary time to calculate the electronic ground state of a system. We will use this ground state then as the initial condition for the calculation of absorption spectra beyond the linear response regime.[14]

To do this we choose a one-dimensional jellium model, which assumes a positive, homogeneous background charge density ρ^+. It is a prototypical system for one-dimensional metals, clusters, and nanostructured materials. It is known to have a rather high correlation energy, and is thus not well described by Hartree–Fock.

The structure of the paper is as follows. The theory of MCTDHF will be presented shortly in Sec. II, in order to introduce notations and concepts. The same section sketches the method of natural potentials, which is essential for an efficient integration of the equations of motion. Section III presents the applications and Sec. IV summarizes this paper. Some details of the implementation have been gathered in an appendix. We will use atomic units throughout, if not stated otherwise.

II. THEORY

A. The MCTDHF method

The following Hamiltonian describes the N-electron system, treated within the fixed-nuclei approximation:

$$H=\sum_{i=1}^{N}\frac{p_i^2}{2}+\sum_{i=1}^{N}V_{\mathrm{ext}}(r_i)+\sum_{i>j}^{N}V_{e/e}(r_i,r_j). \tag{1}$$

Here, N is the number of electrons, $x_i=(r_i,s_i)$ is the combined position and spin variable of the ith electron, V_{ext} the external potential, and $V_{e/e}$ the electron-electron repulsion. In the one-dimensional model,[5,15] r_i is the coordinate along which electron i is allowed to move. In the following we will

 © 2005 American Institute of Physics

Downloaded 21 Nov 2007 to 141.89.199.236. Redistribution subject to AIP license or copyright; see http://jcp.aip.org/jcp/copyright.jsp

sometimes use the abbreviation $h=p_i^2/2+V_{\text{ext}}(r_i)$ for the single particle Hamiltonian.

We screen the potential in order to avoid the artificial Coulomb singularity in one dimension[15] according to

$$V_{e/e}(r_i,r_j)=\frac{1}{\sqrt{(r_i-r_j)^2+a}}, \tag{2}$$

where for the screening parameter we choose $a=1$.

The jellium model consists of a constant positive background charge density ρ^+, extending over the interval $[-L,L]$, which produces the external potential

$$V_{\text{ext}}(r_i)=-\int \frac{\rho^+(R)dR}{\sqrt{(r_i-R)^2+a}}. \tag{3}$$

The value of ρ^+ within the interval can be derived from the condition that the system should not have a net charge: $\rho^+=N/(2L)$.

The evolution of the system is described by the N-electron, time-dependent wave function $\Psi(x_1,\ldots,x_N,t)$. This is expanded into a sum of Hartree products, which in turn are made of spin orbitals (or single particle functions) φ_j,

$$\Psi(x_1,\ldots,x_N,t)=\sum_{j_1=1}^{n}\cdots\sum_{j_N=1}^{n}A_{j_1\cdots j_N}(t)\prod_{k=1}^{N}\varphi_{j_k}(x_k,t). \tag{4}$$

The indices j_i enumerate the n spin orbitals $\varphi_j(t)$ (= the molecular orbitals) used for the representation of the wave function. The Pauli principle requires the coefficient tensor $A(t)$ to be antisymmetric. From this it follows that, of a total of n^N number of elements, $n!/(n-N)!$ are nonzero, and only $\binom{n}{N}$ are independent. From a quantum chemical point of view one usually thinks of an expansion of Ψ by means of Slater determinants. Equation (4) can be resummed to give determinants whose coefficients are just the independent elements of A. The time-dependent orbitals themselves are, in turn, defined on a time-independent, primitive basis. In standard quantum chemistry, this is typically an atomic orbital basis, or a plane wave basis in solid state physics. Here we use a grid basis consisting of N_G grid points. Of course, the representation of the wave function according to Eq. (4) is only approximate, as long as the expansion length n is finite.

The time dependence of the spin orbital φ and the coefficients A can be deduced from the Dirac–Frenkel variational principle. As this has been done in detail elsewhere,[8] it suffices to say that the equations of motion are not unique because phase factors can be moved from A to the φ's, and vice versa. We will be dealing in this paper specifically with two versions.

In order to express coefficients and orbitals in a concise form, we have to introduce some auxiliary quantities. First, we introduce a vector of all orbital φ_k, denoted by $\vec{\varphi}$. A Hartree product will be abbreviated by $\Phi_J=\varphi_{j_1}(x_1,t)\cdots\varphi_{j_N}(x_N,t)$, where J is a composite index of N indices j_k. We follow Ref. 8 and define single-hole functions,

$$\Psi_j=\sum_{j_2}\cdots\sum_{j_N}A_{jj_2\cdots j_N}\prod_{k=2}^{N}\varphi_{j_k}(x_k,t), \tag{5}$$

in order to get compact expressions for the single particle density matrix

$$\rho_{jl}=\langle\Psi_j|\Psi_l\rangle, \tag{6}$$

and the mean fields

$$\langle V_{e/e}\rangle_{jl}=\langle\Psi_j|V_{e/e}|\Psi_l\rangle. \tag{7}$$

Finally, we define the operator P to be a projector on the space spanned by the orbitals:

$$P=\sum_{j=1}^{n}|\varphi_j\rangle\langle\varphi_j|. \tag{8}$$

Having done this, we can write down the equations of motion.

In a first version, we use,

$$\dot{A}_J=-i\sum_L\langle\Phi_J|V_{e/e}|\Phi_L\rangle A_L, \tag{9}$$

$$\dot{\vec{\varphi}}=-i[h+(1-P)\rho^{-1}\langle V_{e/e}\rangle]\vec{\varphi}. \tag{10}$$

Because of the ordering of operators, we will refer to this set of equations henceforth as hP version.

In a second version, henceforth called Ph, we use,

$$\dot{A}_J=-i\sum_L\langle\Phi_J|H|\Phi_L\rangle A_L, \tag{11}$$

$$\dot{\vec{\varphi}}=-i(1-P)[h+\rho^{-1}\langle V_{e/e}\rangle]\vec{\varphi}. \tag{12}$$

A comparison of the two versions yields the following two differences. First, in Eq. (9) the coefficients $A_J(t)$ oscillate with a frequency proportional to the electron-electron interaction, whereas in Eq. (11) the full Hamiltonian appears. Second, and conversely, the projector in Eq. (12) restricts the evolution of the orbitals much more than in Eq. (10). In other words, going from version 1 to version 2 shifts part of the dynamics from the orbitals to the coefficients. This is why version 2 is more suitable for the constant mean field algorithm[8] than version 1, which is usually used for variable mean field calculations. This difference has consequences for the numerical solution of the differential equations, see Sec. III.

The variational principle assures that the representation of the wave function [Eq. (4)] is optimal at all times. Both the coefficients as well as the orbitals are optimized. In this sense, the method presented here is an explicitly time-dependent version of CASSCF/MCSCF (MCSCF—multiconfiguration self-consistent field), which we will refer to as the MCTDHF or the TD-CASSCF method henceforth. If $n=N$ the TD-HF case, and if $n=N_G$ the full-CI limit is obtained. In between, the method can be improved systematically.

Downloaded 21 Nov 2007 to 141.89.199.236. Redistribution subject to AIP license or copyright; see http://jcp.aip.org/jcp/copyright.jsp

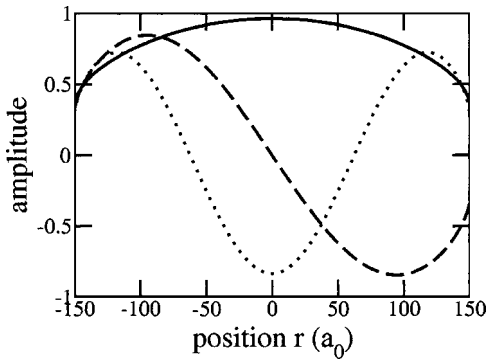

FIG. 1. First three natural potentials $v_i(r)$ for the potential given in Eq. (2). Solid line, $i=1$; dashed line, $i=2$; and dotted line, $i=3$. The natural potentials are similar to plane waves, but not identical to them, because of the screening of the Coulomb potential [Eq. (2)].

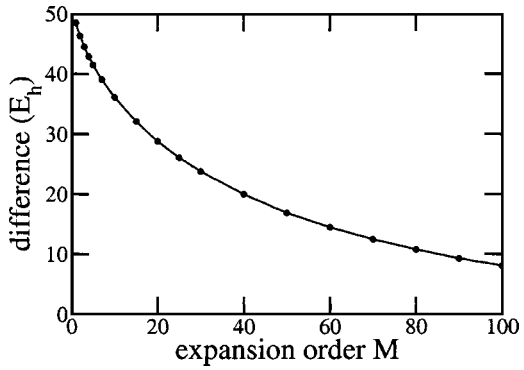

FIG. 2. Difference between the approximate and the exact potential as a function of the natural potential expansion size M.

B. Natural potentials

As in almost all kinds of quantum chemical calculations, a large part of computation time is spent with the evaluation of what we call the mean fields. [The two electron integrals in molecular orbital basis]. A significant speed-up can be obtained with the expansion

$$V_{e/e}(r_1,r_2) \approx \tilde{V}_{e/e}(r_1,r_2) = \sum_{i=1}^{M} v_i(r_1)v_i(r_2), \tag{13}$$

which changes in a one-dimensional model a two-dimensional integration into $2M$ one-dimensional integrations. This is advantageous as long as $2M$ is smaller than the size of the primitive basis, on which the orbitals are defined. The $v_i(r)$ are called natural potentials. A scheme which gives the optimal expansion of this kind, the so-called natural potential expansion, can be found, e.g., in Ref. 8. In general, the natural potentials $v_i(r)$ are different for every degree of freedom. That this is not so in Eq. (13) is a consequence of the symmetry of the Coulomb potential.

The first three natural potentials $v_i(r)$ $(i=1,2,3)$ are shown in Fig. 1. They are very similar, but not identical, to plane waves. This is not surprising, because integrals of the kind of Eq. (7) are often solved with a Fourier method in standard quantum chemical calculations. The deviation from plane waves originates from the form of Coulomb screening that we employed.

The approximate potential $\tilde{V}_{e/e}$ becomes better with increasing expansion length. The difference, calculated according to

$$\left[\sum_{i=1}^{N_G}\sum_{j=1}^{N_G}[V_{e/e}(r_{1i},r_{2j}) - \tilde{V}_{e/e}(r_{1i},r_{2j})]^2\right]^{1/2}, \tag{14}$$

where r_{1i} and r_{2j} are grid points, and $N_G=512$ is the number of points, is shown in Fig. 2.

One should be careful to distinguish the difference, as defined in the expression above, from the "error" of the potential energy surface, which should be defined on the basis of quantum mechanical energy expectation values. That error has a much more comfortable dependence on M, as will be discussed later.

III. APPLICATIONS

As we have mentioned in the Introduction, we will use the jellium potential to model a one-dimensional metal. The system parameters will be $L=50a_0$ and $N=6$ electrons. This results in a typical work function of 4.9 eV, calculated with Koopmans' theorem and a restricted Hartree–Fock ansatz.

For simplicity, we will work in the following with restricted orbitals, too, and consider only singlet states. We will adopt the usual CASSCF notation (N,K), with the number of electrons and *spatial* orbitals (2K=n), respectively. The differential equations (9)–(12) have been solved with an adaptive step size Runge–Kutta integrator[16] of order 8.

The orbitals are represented on a grid of 512 points in position space from $-150a_0$ to $150a_0$. In this basis it is trivial to evaluate matrix elements of potential energy operators. The kinetic energy is evaluated using the Fourier method.[17]

We will start our discussion with the propagation in imaginary time/relaxation technique,[18] for two reasons. First, we need an initial wave function for the real time propagation. This will often be the ground state of the system. Second, the propagation in imaginary time can be interesting in its own right, because it is an alternative way to solve the time-independent electronic Schrödinger equation. It reformulates the problem from an implicit system of equations to an explicit one. This might entail fewer numerical problems and circumvents the notorious problem of the choice of configurations.

A. Imaginary time propagation: relaxation

Propagation in imaginary time means that the real time variable t in the propagator e^{-iHt} is replaced by $\tau=it$ in the Schrödinger equation, i.e., $\Psi(\tau)=e^{-H\tau}\Psi(0)$, where $\Psi(0)$ is an initial wave function. Then the formal solution can be written as

$$\Psi(\tau) = c_0 e^{-E_0\tau}\Psi_0 + c_1 e^{-E_1\tau}\Psi_1 \ldots, \tag{15}$$

where E_i and Ψ_i refer to the N-electron eigenvalues and eigenfunctions of the full electronic Hamiltonian, respectively. Because $E_0<E_1<E_2<\ldots$, the fraction c_0^2 of the ground state in Ψ increases with τ, and becomes 1 for $\tau \to \infty$. Thus, the method should lead to $\Psi \approx \Psi_0$, if the wave function is renormalized at suitable intervals.

Downloaded 21 Nov 2007 to 141.89.199.236. Redistribution subject to AIP license or copyright; see http://jcp.aip.org/jcp/copyright.jsp

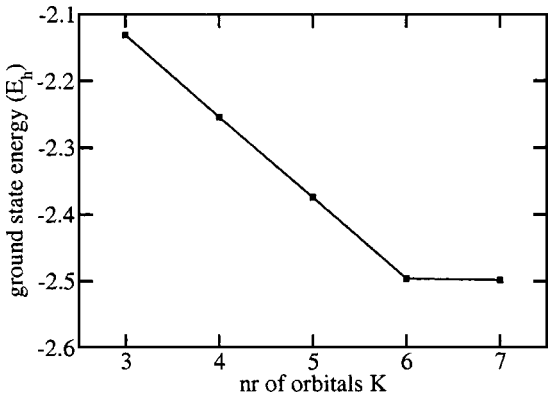

FIG. 3. Lowest energy obtained by imaginary time propagation for different numbers of spatial orbitals K, using time-dependent CASSCF (6,K). The full-CI limit is almost reached as soon as sixfold excitations are accounted for. The fact that the curve does not flatten already for smaller K shows that we are dealing with a highly correlated system.

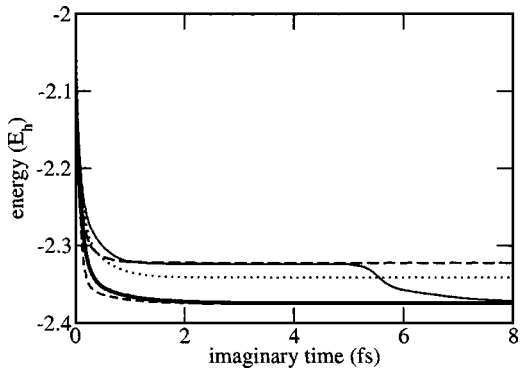

FIG. 4. Energy expectation values for different initial conditions of the propagation in imaginary time. Thick line, lowest energy initial determinant; others, initially excited determinants, see text.

Let us now discuss the choice of initial conditions, i.e., the choice of $\Psi(0)$. The relaxation procedure described above is in general only successful if the ground state Ψ_0 has a sufficiently large amplitude in the initial wave function. We tried several *ansätze*, and found that the following procedure gives good results. Given the boxlike shape of the jellium potential, we used the lowest K eigenfunctions of an infinite square well of length $2L$, i.e., sine and cosine functions φ_i', for the spatial orbitals. From each of them two spin orbitals are constructed by multiplication with spin functions. We choose to start with a single determinant, therefore one of the $\binom{n}{N}$ elements equals $1/\sqrt{N!}$, and all other independent elements of $A(t)$ are zero. Version two (Ph) of the equations of motion has been found to converge more reliably than version one. The former got its name because the slowly varying orbitals result in a slowly varying mean field, which could be kept constant over several time steps in nuclear dynamics applications of MCTDH. We tried this kind of numerical approximation [in a first-order version, see (Ref. 8)] as well, but found that it introduces an error which is too big for electronic structure calculations.

The energy of the ground state wave function that is found decreases with the number of orbitals (the size of the active space) according to the variational principle. Figure 3 shows the lowest energy found via propagation in imaginary time as a function of the number of space orbitals. The case $K=3$ corresponds to a TD-RHF (RHF—restricted Hartree–Fock) calculation, and indeed this method reproduces ($-2.130\,91E_h$) the Hartree–Fock energy of a time-independent calculation ($-2.130\,88E_h$). Additional orbitals decrease the energy significantly. A system of six electrons can at most be excited sixfold, so that for $K=6$ this limit is reached. In fact, we find that another orbital lowers the energy only by $1.7\mathrm{mE}_h$. In the case of four electrons we find the same sharp edge at $K=4$, and a nearly constant energy for $K=4,\ldots,7$.

From this we can conclude that the correlation energy is about 15% of the ground state energy for the six electron system. This high value is a consequence of the one dimensionality of our system, albeit a welcome one, because it allows us to test the method under difficult conditions.

However, the method does not converge to the ground state for every choice of initial wave function $\Psi(0)$. Figure 4 shows the energy expectation value as a function of imaginary time for seven different initial determinants for the case TD-CASSCF (6,5). There are $\binom{10}{6}=210$ determinants here, of which 10 are pure singlet states. 110 determinants have an unequal number of spin up and down electrons, so they cannot be combined linearly to give a singlet state, and are therefore neglected in the propagation. The most natural choice for initial state is of course the determinant which is constructed from the three lowest particle-in-a-box spatial orbitals, i.e., $\Psi(0)=\mathcal{A}|\varphi_1'\overline{\varphi}_1'\varphi_2'\overline{\varphi}_2'\varphi_3'\overline{\varphi}_3'\rangle$. (This denotes an antisymmetrized Hartree product.) The time evolution of the energy of the system is shown as a black, thick line in Fig. 4. Using the usual CI notation,[19] the other initial configurations are $\Psi_{3\overline{3}}^{4\overline{4}}$ $\Psi_{3\overline{3}}^{5\overline{5}}$, $\Psi_{2\overline{2}}^{5\overline{5}}$, and $\Psi_{2\overline{2}3\overline{3}}^{4\overline{4}5\overline{5}}$. It is not predictable which initial state ends up in the ground state. Unfortunately, this is not because the ground state wave function is not contained in them. The mutual overlap of the final states is of the order of a few percent. We also observed this behavior of imaginary time propagation with MCTDH for nuclei. Another problem is that, in rare cases, the energy might stabilize on a higher plateau, which feigns a convergence. However, both problems can be solved by repeating the calculation with somewhat different initial conditions. The quality of the wave function that is obtained in this way can be checked with a short time propagation in real time. If a superposition of eigenstates has been produced, the position expectation value will not be constant. Another possibility to easily check the results is to use different functional forms for the initial orbitals, e.g., Hermite–Gauss functions.

During imaginary time propagation, the electron density relaxes together with the energy. It adapts itself to the potential well, as can be seen in Fig. 5 for the CAS(6,6) case. For values of L that are quite large (here: $50a_0$), we find that the six electrons form a density with six maxima, corresponding to a "charge density wave." These maxima are very close ($<1a_0$) to the equilibrium positions that "classical" electrons would take. For narrow wells, say $L\ll 20a_0$, the six maxima collapse to three. The exact mechanism of this behavior is as yet unclear.

CASSCF calculations converge to the full CI limit, when only enough configurations are chosen, or, in other words,

Downloaded 21 Nov 2007 to 141.89.199.236. Redistribution subject to AIP license or copyright; see http://jcp.aip.org/jcp/copyright.jsp

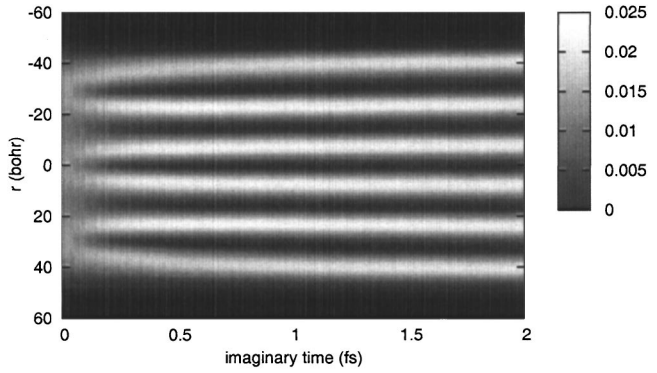

FIG. 5. Relaxing electron density in the (6,6) case, in a_0^{-1}.

when the active space is large enough. A quantitative measure for this are the natural populations, i.e., the populations of the eigenfunctions of the reduced one-particle density operator ρ. We are using the normalization $\mathrm{Tr}\,\rho=N$. Figure 6 shows results for the (6,7) case. In the figure, always two curves lie exactly on top of each other because we are using restricted spin orbitals. Only the six spin orbitals which build the initial determinant are occupied at time $t=0$. At the end of the relaxation process all fourteen spin orbitals within the active space contribute significantly to the wave function. This again shows the high degree of correlation in this system.

We want to conclude this section with another look at the dependence of the ground state energy on the natural potential expansion size M, see Eq. (13) and Fig. 2. While the difference between the approximate and the exact potential falls off only very slowly, we find a completely different functional dependence of the ground state energy on M. Figure 7 shows this dependence for the CAS(6,4) case. The energy grows because more correlation is taken into account, until a plateau is reached. For $M \geqslant 50$ convergence in the energy is almost achieved, although $\tilde{V}_{e/e}$ approaches the exact potential much more slowly. Because this is much less than N_G, we obtain a significant speed up of the calculations. For values $M<30$ we find an irregular behavior.

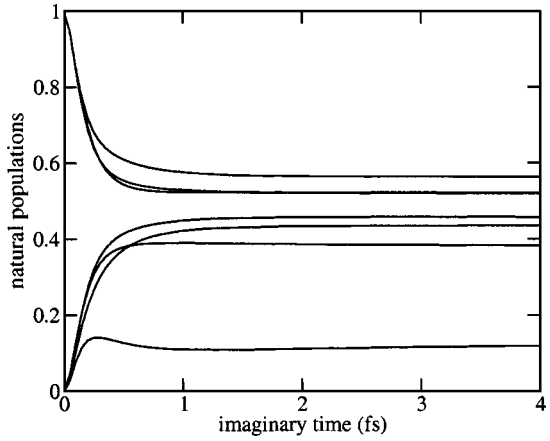

FIG. 6. Natural Populations for the (6,7) case. Always two lines lie exactly on top of each other, because we use the restricted formalism. The energy is much better converged than the lowest final value of about 0.12 indicates.

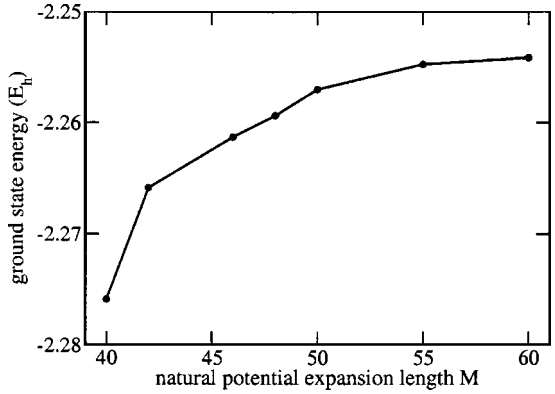

FIG. 7. The energy expectation value as a function of the size of the natural potential expansion. Compared to Fig. 2, the convergence is much faster.

B. Real time propagation

We will now use the MCTDHF approach to calculate the absorption spectrum of the jellium system. The spectrum is obtained from the time-dependent expectation value of the dipole operator

$$\langle \mu \rangle(t) \propto \langle \Psi(t)|r_1|\Psi(t)\rangle \tag{16}$$

via a Fourier transform[20]

$$\sigma(\omega) \propto \omega \int \langle \mu(t)\rangle e^{i\omega t} dt. \tag{17}$$

We create the electronic wave packet $\Psi(t)$ with an ultrashort laser pulse

$$F(t) = \begin{cases} F_0 \sin^2(\pi t/l_p)\cos(\omega_p t), & 0 \leqslant t \leqslant l_p \\ 0, & t > l_p \end{cases}. \tag{18}$$

The field strength is $F_0=0.03\mathrm{mE}_h/(e_0 a_0)$, the width of the sine-square envelope function is $l_p=15$ fs, and the mean laser frequency $\omega_p=0.025\mathrm{E}_h/\hbar$. From this follows an oscillation period of the field of about 8 fs, so that we are dealing with a two-cycle pulse. The resulting spectral width is $8\mathrm{mE}_h$, or one-third of the mean frequency. This was chosen because we want to cover a good range of the lower frequencies. The system is initially in the ground state Ψ_0, obtained by the procedure of the preceding section. The dipole expectation value can then be computed easily, as it is just a single particle quantity.

We propagated the system for 250 fs, and for the (6,3), (6,4), and (6,5) ground states. The absorption spectra are then calculated by Fourier transform of the dipole expectation value for $15\ \mathrm{fs} \leqslant t \leqslant 250$ fs, after a cosine window function has been applied. Figure 8 shows the result. The intensity has been normalized so that the highest peak has intensity one. Its position corresponds to the first excitation energy, which we affirmed by changing the central frequency and field strength. Further, we see that the influence of the size of the active space on this energy difference is much smaller than on the total ground state energy. The width of the peaks and the small neighboring maxima are solely due to the finite propagation time. It should be noted that the excitation energy is smaller than the energy difference be-

Downloaded 21 Nov 2007 to 141.89.199.236. Redistribution subject to AIP license or copyright; see http://jcp.aip.org/jcp/copyright.jsp

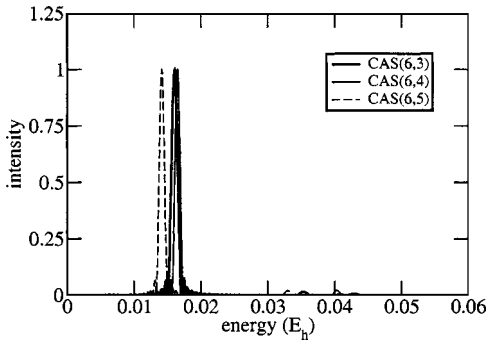

FIG. 8. Absorption spectra of the jellium system for different sizes of the active space.

tween the final states in Fig. 4, which supports the possibility of a "trapping" of the propagation in a band of excited states.

Let us now turn to the performance of the method. It is difficult to find a simple scaling law for medium numbers of N and n, because different parts of the algorithm behave very differently. The most time-consuming task is the calculation of the mean fields, where a sum over all nonzero elements $[n!/(n-N)! \propto n^N]$ of A appears. For the (6,7) case, the coefficient tensor A has 7.5×10^6 elements, of which 2.2×10^6 are nonzero, and 3003 are independent. This is of the same order of magnitude as the biggest quantum dynamical calculations for nuclei done so far[9] with the MCTDH method. We found that the relative, average CPU times are 1, 15.6, and 194 for the (6,3), (6,4), and (6,5) cases. This corresponds to a polynomial increase according to $n^{6.2}$, which could approximately be expected.

The real time propagations above have been done with version one (hP) of the equations of motion. We found that it is generally 50% faster (for this kind of problem) than the (Ph) version.

IV. SUMMARY AND OUTLOOK

We studied the suitability of the MCTDHF method for quantum chemical calculations. The task to find the ground state energy/wave function is an initial value problem, which is easier to solve than implicit systems of equations. However, the calculation of mean fields etc. has to be done at each time step, so that this method will probably be restricted to systems smaller than those that can be treated with the time-independent approach. However, it is a convenient method to prepare initial wave functions for real time wave packet propagations. Problems with an explicit time dependence are the real strength of the method. The two versions of the equations of motion show different adequacy for propagations in imaginary time (Ph) and real time (hP). A systematic study of the calculation of excited states via propagation in imaginary time is under way. The number of possible real time applications is very large; they include correlated electron motion under the influence of electromagnetic fields, transport phenomena, control of chemical processes, to name a few.

ACKNOWLEDGMENTS

M.N. thanks Hans-Dieter Meyer for stimulating discussions. This work was funded by the Deutsche Forschungsgemeinschaft, under Grant No. SPP 1145.

APPENDIX: DETAILS OF IMPLEMENTATION

a. Coefficients. It is not necessary to solve the differential equations (9) and (11) for all n^N elements because one can reconstruct most of them from a small number of independent composite indices. This does not come for free, however, but has to be paid for by a rather complex scheme of bookkeeping. If, e.g., (1 2 3 8 10 12) is such an independent index, then it has to be determined how many permutations are necessary to convert, say, (1 12 2 8 3 10) into the former. Such operations must be done quite frequently. A further reduction of the computational effort can be achieved if we look at equations where matrix elements of Hartree products must be calculated. For example,

$$\dot{A}_J = -i\sum_L \langle\Phi_J|H|\Phi_L\rangle A_L. \tag{A1}$$

Here, it is not necessary to let the sum over L run over all nonzero elements A_L, because many inner products vanish because of the spin part of the orbitals. It suffices to perform the sum over all nonzero elements once before the propagation begins. The addresses of the corresponding independent composite indices and the number of necessary permutations can then be recorded and stored in an auxiliary array.

b. Single Electron Density Matrix. If we rewrite Eq. (6) in more detail we find that

$$\rho_{jl} = \sum_{j_2,\cdots,j_N=1}^{n} A^*_{jj_2\cdots j_N} A_{lj_2\cdots j_N}, \tag{A2}$$

because of the orthogonality of the spin orbitals. This rather large sum reduces to a sum over all independent (ordered) indices $(j_2\cdots j_N)$, because the number of permutations for both coefficients is the same, so that the effective sign is always $+1$. The result then has to be multiplied by $(N-1)!$.

c. Mean Fields. The mean fields can be divided into two parts because the position and spin variables of the "first" degree of freedom are missing in the definition [Eq. (5)] of the single-hole wave functions Ψ_j. Part one contains all parts of $V_{e/e}$ which depend on x_1 and an arbitrary second one x_s, part two contains all other combinations (x_s,x_t),

$$\langle V_{e/e}\rangle_{jl} = \sum_{j_2,\ldots,j_N}\sum_{l_2,\ldots,l_N} A^*_{jj_2\cdots j_N} A_{ll_2\cdots l_N} \sum_{i=1}^{M} v_i(x_1) \times \sum_{s=2}^{N} \langle j_2\cdots j_N|v_i(x_s)|l_2\cdots l_N\rangle \tag{A3}$$

$$+ \sum_{j_2,\cdots,j_N}\sum_{l_2,\cdots,l_N} A^*_{jj_2\cdots j_N} A_{ll_2\cdots l_N} \times \sum_{i=1}^{M}\sum_{s=2}^{N-1}\sum_{t=s+1}^{N} \langle j_2\cdots j_N|v_i(x_s)v_i(x_t)|l_2\cdots l_N\rangle. \tag{A4}$$

Downloaded 21 Nov 2007 to 141.89.199.236. Redistribution subject to AIP license or copyright; see http://jcp.aip.org/jcp/copyright.jsp

The upper term is the same for all s, so that we only need to calculate the result for $s=2$ and multiply it by $(N-1)$. The lower term is the same for all pairs (s,t) so that we need only to calculate the $(s=2,\ t=3)$ case, and multiply the result by $(N-1)(N-2)$.

[1]E. Runge and E. K. U. Gross, Phys. Rev. Lett. **52**, 997 (1984).
[2]F. Calvayrac, P.-G. Reinhard, E. Suraud, and C. A. Ullrich, Phys. Rep. **337**, 493 (2000).
[3]K. C. Kulander, Phys. Rev. A **36**, 2726 (1987).
[4]M. S. Pindzola, P. Gavras, and T. W. Gorczyca, Phys. Rev. A **51**, 3999 (1995).
[5]T. Klamroth, Phys. Rev. B **68**, 245421 (2003).
[6]D. Hegarty and M. A. Robb, Mol. Phys. **38**, 1795 (1979).
[7]H.-D. Meyer, U. Manthe, and L. S. Cederbaum, Chem. Phys. Lett. **165**, 73 (1990).
[8]M. H. Beck, A. Jäckle, G. A. Worth, and H.-D. Meyer, Phys. Rep. **324**, 1 (2000).
[9]M. Nest and H.-D. Meyer, J. Chem. Phys. **119**, 24 (2003).
[10]H.-D. Meyer and G. A. Worth, Theor. Chem. Acc. **109**, 251 (2003).
[11]J. Zanghellini, M. Kitzler, C. Fabian, T. Brabec, and A. Scrinzi, Laser Phys. **13**, 1064 (2003).
[12]T. Kato and H. Kono, Chem. Phys. Lett. **392**, 533 (2004).
[13]U. Manthe and F. Matzkies, Chem. Phys. Lett. **252**, 71 (1996).
[14]J. Olsen and P. Jorgensen, J. Chem. Phys. **82**, 3235 (1985).
[15]R. Grobe and J. H. Eberly, Phys. Rev. A **48**, 4664 (1993).
[16]E. Hairer, S. P. Norsett, and G. Wanner, *Solving Ordinary Differential Equations I*, 2nd ed. (Springer, Berlin, 1993).
[17]J. A. Fleck, J. R. Morris, and M. D. Feit, Appl. Phys. **10**, 129 (1976).
[18]R. Kosloff, J. Phys. Chem. **92**, 2087 (1988).
[19]A. Szabo and N. S. Ostlund, *Modern Quantum Chemistry* (Dover, New York, 1996).
[20]G. C. Schatz and M. A. Ratner, *Quantum Mechanics in Chemistry* (Prentice-Hall, New Jersey, 2002).

Downloaded 21 Nov 2007 to 141.89.199.236. Redistribution subject to AIP license or copyright; see http://jcp.aip.org/jcp/copyright.jsp